TELKOMNIKA, Vol.13, No.3, September 2015, pp. 870~879
ISSN: 1693-6930, accredited A by DIKTI, Decree No: 58/DIKTI/Kep/2013
DOI: 10.12928/TELKOMNIKA.v13i3.1974

Enhanced Channel Estimation Algorithm for Dedicated Short-Range Communication Systems

Xiang Li[1]*, Fuqiang Liu[1], Nguyen Ngoc Van[2]
[1]School of Electronics and Information Engineering, Tongji University, Shanghai, China
[2]School of Electronics and Telecommunications, Hanoi University of Science and Technology, Hanoi, Vietnam
*Corresponding author, e-mail: lixiang_277@163.com

Abstract

The Dedicated Short-Range Communication (DSRC) has been widely accepted as a promising wireless technology for enhancing traffic safety. In such DSRC-based vehicle-to-vehicle (V2V) communication systems, because of the extremely time-varying characteristic of wireless propagation channels, accurate channel estimation is essential for reliable information exchange between vehicles. In this paper, the characteristics of the propagation channel and several traditional channel estimation schemes for V2V communications are reviewed. Then, a delay-based channel-frequency-response decomposition scheme is proposed to estimate and predict the double-selective V2V channel while adhering to the IEEE 802.11p standard. The proposed method achieves a more favorable performance than the traditional methods in V2V scenarios by combining the least square estimation in the frequency domain with the linear prediction in time domain. The performance advantages of the proposed scheme are verified by the simulation results from three typical scenarios. Furthermore, a reference design on a field-programmable gate array for the proposed channel estimation scheme is presented for the purpose of demonstrating its implementation feasibility and complexity.

Keywords*: dedicated short range communications (DSRC), IEEE 802.11p standard, orthogonal frequency division multiplexing (OFDM), channel estimation*

1. Introduction

Dedicated Short-Range Communications (DSRC) is a wireless communication technique that enhances the safety and efficiency of transportation systems by enabling for a high-speed data exchange between vehicles. The U.S. Department of Transportation has estimated that vehicle-to-vehicle (V2V) communication can be used to manage up to 82% of all crashes arising from unimpaired drivers [1]. Currently, the most common worldwide DSRC standard is the IEEE 802.11p [2], which is based on orthogonal frequency division multiplexing (OFDM) [3]. Due to the high mobility of vehicles, the channels within the vehicular communication scenarios vary significantly in both time and frequency domain. Compared to the indoor channels, the time-varying characteristic of wireless propagation channels is a severe obstacle for reliable packet delivery. We focus on the practical methods for improving the reliability of V2V communications using enhanced channel estimation inherent to the IEEE 802.11p standard.

The V2V channel propagation characteristics differ significantly from those of cellular and indoor stationary channels, especially in terms of their frequency-selectivity, time-selectivity, and associated fading statistics [4,5]. Time-variation results in a short channel coherence time, which causes the channel to change significantly from the start of the packet to the end of the packet. A commercially-available channel estimation scheme for chip set implementation in an indoor environment is the preamble-based least square (LS) [3] estimator. In the V2V communication environment, however, the LS estimator will significantly degrade system performance because it neglects the time-varying characteristic. A simple and accurate method to trace the time-varying channel is a linear interpolation either in the frequency direction only or the time-frequency-direction [6-9]. However, only four sub-carriers are allocated as pilots in the IEEE 802.11p standard, and they are not spaced closely enough to accurately sample the

Received March 25, 2015; Revised June 24 2015; Accepted July 8, 2015

frequency-selective channel. On the other hand, [10] proposed a method that is based on the time-domain differentiation to compensate for the short coherence time of the channel. Although this method is both facile and robust, it requires modification to the IEEE 802.11p standard.

Convolution codes with a short constraint length are used as the channel coding scheme in IEEE 802.11p standard, which means that one can use the already decoded bits as pilots for the remaining packets to improve the channel estimation [11]. Based on this idea, a spectral temporal averaging (STA) estimation scheme is proposed in [12] to trace the time-varying channel. However, knowledge of the radio environment is necessary when using this scheme and this knowledge is normally hard to attain in practice. Considering the high correlation between the channel frequency responses (CFR) for time-adjacent symbols, an estimation scheme that uses preamble-based estimations and constructed data pilots (CDP) is presented in [13]. However, the influence of random noise is not taken into account. Moreover, both the STA and CDP methods use the channel estimation obtained from the previous OFDM symbol to equalize the current symbol, the outdated estimation is no longer valid for the use of the channel equalization in the current OFDM symbol in the fast time-varying channel [14].

We analyze the characteristics of the V2V propagation channels, and review several of the traditional channel estimation schemes in this paper. A delay-based CFR decomposition and prediction (DDP) scheme is then proposed to estimate and predict dynamic V2V channels. The simulation results obtained from three typical V2V communication scenarios demonstrate the favorable DDP scheme performance in terms of the packet error rate (PER) over the traditional methods.

2. System Model

In the IEEE 802.11p standard, two 6.4µs long training symbols (LTSs) are placed in the beginning of each packet to aid in the delivery of the packets, which can be used for the fine timing synchronization, fine frequency offset estimation, and channel estimation. The training symbols are followed by the DATA field, which consists of a variable number of OFDM data symbols that carry the physical layer service data. For all 64 sub-carriers of an OFDM data symbol, 4 sub-carriers spaced 2.1875MHz apart are dedicated as pilot sub-carriers in order to conduct the coherent detection and correct for any residual frequency offset, 48 data sub-carriers are used, and the 12 remaining sub-carriers are reserved. For convenience, consider $\boldsymbol{S_d}$, $\boldsymbol{S_p}$, and $\boldsymbol{S_n}$ as a set of data, pilot, and null sub-carriers, and let $\{\boldsymbol{S}_{\boldsymbol{k}}^{\boldsymbol{i}}\}_{\boldsymbol{k}=0}^{N_c-1}$ be the mapped frequency-domain complex sequence for the ith OFDM symbol ($\boldsymbol{N_c} = 64$ denotes the number of sub-carriers). Moreover, the superscript " $\boldsymbol{i}$ " is used to denote the ith OFDM symbol in a packet, the subscript " $\boldsymbol{k}$ " denotes the kth sub-carrier in a symbol.

In vehicular communications, signals propagate from the transmitter to the receiver via different paths, and the received signal is a superposition of all the waves coming from all directions due to the reflection, diffraction, and scattering caused by buildings, trees, vehicles, and other obstacles. All of these waves are attenuated, delayed, and phase-shifted replicas of the transmitted signal. This effect is known as *multipath* propagation, which results in inter-symbol interference. Another negative influence of the V2V channel on the transmitting signal is the *Doppler* effect caused by the rapid movement of both the transmitter and receiver vehicles, which results in inter-subcarrier interference.

Let τ_l , $\Delta\omega_l$ and $\boldsymbol{a_l}$ be respectively the propagation delay (measured by using the sampling period), the normalized *Doppler* radian frequency shift, and the attenuation quotient of the lth incident path. Considering that the *Doppler* shift, $\Delta\omega_l$, is very small, the received replicas of the ith OFDM symbol from the lth path can be written as:

$$R_{k,l}^{i} \approx a_l e^{-j\Delta\omega_l Ni} e^{-j\omega_0 k\tau_l} S_k^i, \quad 0 \le k < N_c \,, \tag{1}$$

Where $\omega_0 = 2\pi / \boldsymbol{N_c}$ be the normalized radian frequency. Consequently, the received samples in the frequency domain in the receiver are the sum of the samples from all of the paths plus the noise, written as:

$$\hat{R}_k^i = S_k^i \sum_{l=1}^{L} a_l e^{-j\Delta\omega_l N i} e^{-j\omega_0 k\tau_l} + W_k^i, \quad 0 \le k < N_c \tag{2}$$

Where W_k^i is the additive white Gaussian noise (AWGN) superposed to the ith symbol. Therefore, the CFR of the radio channel for the ith received symbol can be expressed as:

$$H_k^i = \sum_{l=1}^{L} a_l e^{-j\Delta\omega_l N i} e^{-j\omega_0 k\tau_l}, \quad 0 \le k < N_c. \tag{3}$$

Compared to traditional indoor channels, due to the *Doppler* shifts, the CFR of the V2V channel significantly varies. Channel estimation should be updated in the receiving process.

3. Channel Estimating and Predicting

3.1. Conventional Channel Estimation Schemes

As mentioned previously, two LTSs are put in front of each packet to perform fine synchronization as well as channel estimation according to the physical layer of the IEEE 802.11p standard. Assuming that the received frequency-domain LTSs are $\hat{R}_k^{T_1}$ and $\hat{R}_k^{T_2}$, the LS channel estimator can be expressed as [3]:

$$\hat{H}_k^i = \frac{\hat{R}_k^{T_1} + \hat{R}_k^{T_2}}{2S_k^T} = H_k^i + \frac{W_k^{T_1} + W_k^{T_2}}{2S_k^T}, \quad 0 \le k < N_c, \tag{4}$$

Where S_k^T is the predefined LTS. Next, the estimated CFR is used to equalize the subsequent data symbols for the entire packet. However, in a V2V scenario, the *Doppler* shift can reach up to 1400Hz [4] (0.07rad/symbol). Consequently, the CFR is highly variable, as detailed in Equation (3). Equalizing the time-varying channel with a constant CFR will significantly deteriorate the entire system performance. The CFR estimation must be updated symbol by symbol to adapt to the continually evolving propagation channel.

A common channel updating scheme for the OFDM system with a comb-type pilot is the interpolation technique [6], in which the CFR in the pilot sub-carriers is estimated using the LS estimator symbol by symbol, then the CFR in the data sub-carriers is obtained by interpolation. The maximal multipath propagation delay, τ_{max}, can be up to 800ns (8 samples) [4] in a V2V scenario. According to the Nyquist sampling theorem, the amount of sub-carrier spacing between the pilots in frequency domain D_p must be small enough, that is, $D_p \le N_c / (2\tau_{max}) = 4$ must be satisfied [15]. However, $D_p = 14$ in the IEEE 802.11p standard. Obviously, an acceptable performance cannot be achieved using the interpolation techniques.

One potential set of methods for channel estimating and tracing are the data-pilot-aided schemes, in which the feedback from all the de-mapped or decoded data information is used to construct data pilots and update the channel estimation over the receiving process of a packet. If we consider $\hat{S}_k^i$ as the reconstructed data pilot for the kth sub-carrier of the ith symbol, the CFR estimation is:

$$\hat{H}_k^i = \frac{\hat{R}_k^i}{\hat{S}_k^i} = H_k^i + \frac{W_k^i}{\hat{S}_k^i}, \quad k \in \mathbf{S}_d \text{ or } \mathbf{S}_p. \tag{5}$$

This estimation is used to equalize the $(i+1)$th symbol. However, the system performance suffers from the error propagation problem, as the incidentally incorrect estimation of CFR caused by noise and interference results in a succession of additional error estimations when it is used to equalize the subsequent symbol.

In order to tackle the error propagation problem, the CDP [13] scheme took the correlation of the channel for time-adjacent data symbols into account. Let $\hat{H}_{k,CDP}^{i-1}$ be the CFR estimation before the ith symbol is received. In the CDP scheme, $\hat{H}_k^i$ and $\hat{H}_{k,CDP}^{i-1}$ are used to equalize the $(i-1)$th received data symbol,

$$\hat{S}_{k,CDP}^{i-1} = \frac{\hat{R}_k^{i-1}}{\hat{H}_{k,CDP}^{i-1}}, \quad \hat{S}_k^{i-1} = \frac{\hat{R}_k^{i-1}}{\hat{H}_k^i}, \quad k \in \mathbf{S}_d \; or \; \mathbf{S}_p . \tag{6}$$

Because of the correlation between time-adjacent CFRs, $\hat{S}_{k,CDP}^{i-1}$ and $\hat{S}_k^{i-1}$ should be de-mapped to the same constellation points. If this holds true, according to the CDP scheme, the updated channel estimation is $\hat{H}_{k,CDP}^i = \hat{H}_k^i$, otherwise $\hat{H}_{k,CDP}^i = \hat{H}_{k,CDP}^{i-1}$. However, no method currently exists to alleviate the deterioration on the system performance caused by noise in the CDP scheme. In the STA [12] scheme, the estimated CFR $\hat{H}_k^i$ is first obtained using equation (5), and then it is averaged in both the frequency domain and time domain in order to improve the accuracy. The updated channel estimation is:

$$\hat{H}_{k,STA}^i = \left(1 - \frac{1}{\alpha}\right)\hat{H}_{k,STA}^{i-1} + \frac{1}{\alpha}\sum_{\lambda=-\beta}^{\beta} \omega_\lambda \hat{H}_{k+\lambda}^i, \quad k \in \mathbf{S}_d \; or \; \mathbf{S}_p , \tag{7}$$

Where β is an integer parameter that affects the number of sub-carriers averaged in the frequency domain, ω_λ is a set of weighting coefficients that form a unified sum, and α is an updating parameter related to the *Doppler* shift. The parameters α , β , and ω_λ must be determined using the knowledge of the radio environment to achieve an optimum performance, which is extremely difficult to obtain.

Furthermore, the data-pilot-aided schemes introduce two basic problems: the use of outdated channel estimates, and the assumption of correct data detection [15]. In the STA and CDP schemes, the channel estimation obtained from a previous OFDM symbol is used to equalize the current OFDM symbol directly and without the deviation between the two adjacent CFRs is taken into account. In the fast time-varying V2V communication channel, such use of the outdated channel estimation tends to result in improper channel equalization especially in a low SNR regime. For the second problem, if the noise and interference strong enough, the received symbol would be de-mapped to incorrect constellation points, and a cascade of incorrect data detection would be the result when the incorrect-de-mapped data information is used to construct data pilots.

3.2. DDP Channel Estimation Scheme

As previously mentioned, the accuracy of the channel estimation degrades due to the *Doppler* shift and noise superposed on the received signal. Although a well-designed low pass filter [16] is indispensable in the transceiver, it can only be used to filter the out-band noise component. Smoothing the estimated channel coefficients in both the frequency domain and time domain is a valid method for suppressing the noise and reducing the error propagation. Taking noise into account, the estimated CFR is:

$$\hat{H}_k^i = \sum\nolimits_{l=1}^{L} a_l e^{-j\Delta\omega_l Ni} e^{-j\omega_0 k\tau_l} + \bar{W}_k^i, \quad k \in \mathbf{S}_d \; or \; \mathbf{S}_p , \tag{8}$$

Where $\bar{W}_k^i = W_k^i / \hat{S}_k^i$. A true CFR is determined by using the a_l , $\Delta\omega_l$, and τ_l of all the propagation paths. It is practically impossible, however, to estimate all of these parameters. Because that the propagation delays are sampled at a frequency of f_s in discrete time-domain, there are only a few available integers for the normalized propagation delay τ_l , an alternative method is to group the propagation paths by focusing on the differing propagation delays, then estimate and trace the channel coefficients for every paths group. If the maximum propagation delay of all propagation paths is MT_s, the available values for τ_l can be $0,1,\cdots,M$, the estimated CFR for the ith symbol can be rewritten as:

$$\hat{H}_k^i = \sum_{m=0}^{M} b_m^i e^{-j\omega_0 km} + \bar{W}_k^i, \quad k \in \mathbf{S}_d \text{ or } \mathbf{S}_p, \tag{9}$$

Where,

$$b_m^i = \sum_{l=1,\tau_l=m}^{L} a_l e^{-j\Delta\omega_l Ni}, \quad 0 \le m \le M, \tag{10}$$

Is the mth delayed *Doppler* effect (DDE) coefficient for the ith symbol, which is determined by the *Doppler* shifts and attenuation quotients of the propagation paths with a mT_s delay. The DDE vector, which is composed of $M+1$ DDE coefficients, is defined as, $\mathbf{b}^i = [b_0^i, b_1^i, \cdots, b_M^i]$. The CFR for the ith symbol can be determined by using the parameter $\mathbf{b}^i$. Moreover, it takes about 1500µs for a vehicle traveling at 120km/h to pass through a wavelength of the IEEE 802.11p standard signal, during which the propagating environments can be considered stationary. Therefore, the propagation paths and their respective delays and *Doppler* shifts are considered invariant for the duration of several dozens of symbols. Moreover, because the *Doppler* shifts are far smaller than the sampling frequency, according to equation (10), the DDE vector $\mathbf{b}^i$ changes slowly and thus can be more easily estimated and predicted.

Based on the previous discussion, we propose a novel DDP estimation scheme to decompose the estimated CFR by using the propagation delay and predicting the new CFR for the subsequent symbol to receive. The proposed method is a three-step process. In the first step, we focus on the estimation of the DDE vector for the currently-processing symbol in the frequency domain; in the second step, the prediction of the DDE vector for the next symbol to receive can be obtained; and in the third step, the CFR for the next symbol to receive is predicted.

3.3. Estimation of DDE Vector

According to the physical layer of the IEEE 802.11p standard, the 64 sub-carriers are divided into 48 data sub-carriers, 4 pilot sub-carriers, and 12 null sub-carriers. After the reconstructed data pilots are obtained from the currently-processing symbol, we can establish an over-determined equations system with 52 equations and $M+1$ unknown variables by using Equation (5) and (9) to respectively determine the channel coefficients on the data and pilot sub-carriers. Although the LS method can then be used to solve the equations system and obtain an estimation of the unknown DDE vector $\mathbf{b}^i$, an overabundance of resources, such as logic cells and hardware multipliers, is involved in its implementation on a hardware platform like FPGA. An alternative method for practical design is to use the DFT-based algorithm [17, 18], which is easily implemented with an acceptable complexity and resource consumption. However, the problem is the channel coefficients on the null sub-carriers are unavailable, and this lack of information significantly deteriorates the performance of the estimation. In order to tackle this problem, we propose filling the channel coefficients on the null sub-carriers with the corresponding predictions obtained from the previously received symbols. The new constructed CFR estimation is

$$\hat{H}_{k,mix}^i = \begin{cases} \hat{H}_{k,DDP}^{i-1}, & k \in \mathbf{S}_n, \\ \hat{H}_k^i, & k \in \mathbf{S}_d \text{ or } \mathbf{S}_p, \end{cases} \tag{11}$$

Where $\hat{H}_{k,DDP}^i$ denotes the predicted channel coefficient according to the previously received symbols. Consequently, the DDE vector $\mathbf{b}^i$ can be estimated by performing the IFFT on the sequence $\hat{H}_{k,mix}^i$

.

3.4. Prediction of DDE Vector

As aforementioned, if the estimated DDE vector $\mathbf{b}^i$ is used directly to equalize the next symbol, the estimation error is a sum of the bias caused by the changed CFR and the error caused by noise and interference. The traditional data-pilots-aided method can only be used to reduce the error caused by noise, at the expense of neglecting the deviation between the two adjacent CFRs. Because the DDE slowly varies symbol by symbol, according to Equation (10), the following points can be considered to lie in a straight line, where W is defined as the length of the estimation window in the time-domain,

$$(-W,\hat{b}_m^{i,-W+1}),\quad (-W+1,\hat{b}_m^{i-W+2}),\quad \cdots,\quad (-1,\hat{b}_m^{i}),\quad 0\le m\le M\ . \tag{12}$$

Thus:

$$\begin{bmatrix} c_{m,0}^i & c_{m,1}^i \end{bmatrix}\begin{bmatrix} 1 & 1 & \cdots & 1 \\ -1 & -2 & \cdots & -W \end{bmatrix}=\begin{bmatrix} \hat{b}_m^i & \hat{b}_m^{i-1} & \cdots & \hat{b}_m^{i-W+1} \end{bmatrix}\quad 0\le m\le M\ , \tag{13}$$

Where $c_{m,0}^i$ and $c_{m,1}^i$ are the slope and intercept of the aforementioned straight line. The unknown $\{\boldsymbol{c}_{m,0}^{i}\}_{m=0}^{M}$ can be treated as the prediction of the DDE coefficients for the imminent $(\boldsymbol{i}+1)^{th}$ symbol. By solving the over-determined equations set (13), the LS prediction of the DDE coefficients can be written as:

$$\hat{b}_{m,pre}^{i+1}=\frac{2(2W+1)}{W(W-1)}\sum\nolimits_{k=1}^{W}\hat{b}_m^{i-k+1}-\frac{6}{W(W-1)}\sum\nolimits_{k=1}^{W}k\hat{b}_m^{i-k+1},\quad 0\le m\le M\ . \tag{14}$$

Consequently, the prediction of the CFR for the imminent $(i+1)\mathrm{th}$ symbol can be obtained according to the Equation (9).

The assumption that the points listed in Equation (12) lie in a straight line must hold in order to use the DDP scheme. On one hand, a large estimation window W is not applicable for a large *Doppler* shift scenario, despite its favorable performance when accounting for noise and interference. On the other hand, with a very small W, an accurate estimation cannot be achieved due to the negative influence arising from random noise and interference. For practicality, the resource consumption can be reduced by specifying W as an integer to the power of 2, because the multiplier and divider involved can be implemented using a bit shifting operation. Moreover, for the purpose of overcoming the inter-symbol interference arising from inaccuracy in the symbol synchronization, the starting position of each symbol is usually specified to advance the true value several samples in the receiver. The delay for all the propagation paths is enlarged. The parameter M should thus be designed to manage this situation.

For the proposed DDP scheme, both the de-mapped and decoded data can be used to construct the data pilots. With the help of an error-correction function provided by the decoder, the decoded-data-aided scheme (C-DDP) performs better in eliminating error propagation. In the de-mapped-data-aided scheme (M-DDP), the received symbols are de-mapped to their corresponding constellation points, and then used to construct the data pilots. In the decoded-data-aided DDP scheme, however, the received symbols must be de-mapped, de-interleaved, and decoded; they are then recoded, re-interleaved, and re-mapped before the channel estimation.

4. Numerical Results and Discussion

The numerical results obtained from a computer simulation of the performance for the proposed DDP scheme are presented in this section. The channel models adopted in this paper for three typical V2V scenarios, including V2V Expressway Oncoming, V2V Urban Canyon Oncoming and V2V Expressway Same Direction with a wall, are detailed in [4]. The parameters used in our simulation for each of the scenarios are configured as follows.

a) *Estimation window*: W is respectively specified as 1 and 4.
b) *Packet length and modulation*: Two kinds of packet lengths, 100 (600 bytes) and 200 (1200 bytes) symbols, are respectively selected. The modulation regime is QPSK.
c) *Maximum delay*: Considering that the maximal multipath propagation delay in all three simulation scenarios (3-8 samples) and that the latency is intentionally introduced to overcome the inaccuracy symbol synchronization (4-6 samples), the value of M is set at 16 for all the simulation scenarios.
d) *Feedback scheme*: Both the de-mapped-data-aided and decoded-data-aided schemes are evaluated. The prefix C-x and M-x, where the 'x' can be LS [3], STA [12], CDP [13], or DDP, are used to respectively denote the demapped-data-aided and decoded-data-aided schemes for the corresponding estimation method.

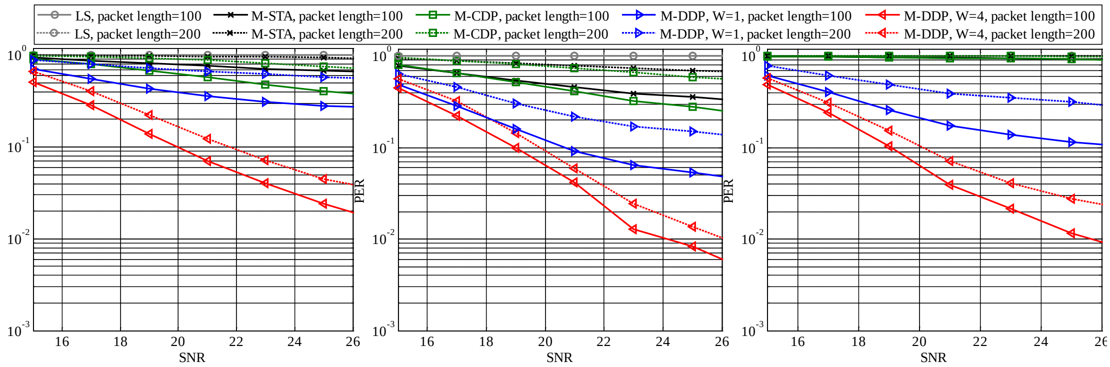

(a) PER with de-mapped-data-aided DDP scheme in V2V Expressway Oncoming scenario

(c) PER with de-mapped-data-aided DDP scheme in V2V Urban Canyon Oncoming scenario

(c) PER with de-mapped-data-aided DDP scheme in V2V Expressway Same Direction with wall scenario

Figure 1. PER with demapped-data-aided DDP scheme for three typical V2V scenarios

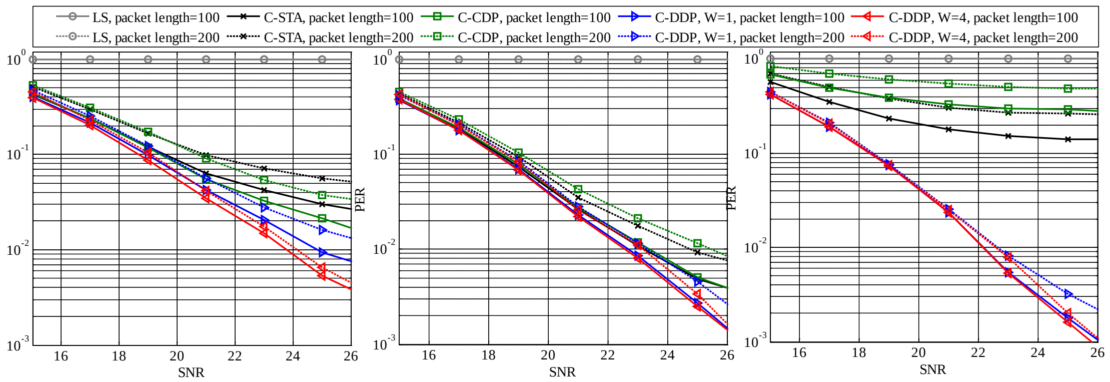

(a) PER with decoded-data-aided DDP scheme in V2V Expressway Oncoming scenario

(b) PER with decoded-data-aided DDP scheme in V2V Urban Canyon Oncoming scenario

(c) PER with decoded-data-aided DDP scheme in V2V Expressway Same Direction with wall scenario

Figure 2. PER with decoded-data-aided DDP scheme for three typical V2V scenarios

Figure 1 and 2 demonstrate the performances of the M-DDP and C-DDP schemes in three typical V2V scenarios. In the V2V Expressway Oncoming scenario, because of the high mobility of the vehicles in an open terrain, the propagation channel is characterized by a large *Doppler* shift, a low overall Rician K factor, and a small path delay. A large *Doppler* shift makes the CFR for consecutive symbols suffer through severe changes. Therefore, as shown in Figure 1(a), compared to the M-STA, M-CDP, and M-DDP with $W=1$ schemes, the proposed M-DDP with $W=4$ scheme performs better by predicting the CFR for an imminent symbol according to the previously estimated CFRs. For the M-DDP scheme, when noise and interference are powerful enough, the received symbol may be de-mapped to incorrect constellation points and cause error propagation. Although the negative influence caused by incorrect mapping can be alleviated by averaging the CFR estimation in both the frequency domain and time domain, a more effective method of solving this problem is to use the C-DDP scheme, by which the influence of incorrect mapping can be eliminated by using an error-correction function of the decoder, as shown in Figure 2(a).

The performance of the proposed DDP scheme in a V2V Urban Canyon Oncoming scenario is presented in Figures 1(b) and 2(b). In this case, the V2V communication experiences a strong multipath fading caused by the numerous reflections from a heavy traffic flow, the nearby buildings, and other environmental factors. Because both the transmitter and receiver are traveling at low speeds, however, the *Doppler* shift is usually relatively small, and thus, the channel changes relatively slowly. In this scenario, the proposed M-DDP scheme still outperforms the M-STA and M-CDP schemes due to its advantages in suppressing noise and managing the negative influence of incorrect mapping. These advantages are weakened when the decoded-data-aided schemes are used. When comparing Figure 2(b) with Figure 1(b), we can see that all of the estimation schemes express almost equally remarkable performances.

In a V2V Expressway Same Direction scenario, both the transmitter and receiver travel at a similarly high speed in the same direction. It seems as though the *Doppler* shift is near zero, because the transmitter and receiver are relatively stationary - however, this is not effectively the case. Although the center frequency of the *Doppler* shift is very small indeed, the fading *Doppler* (the bandwidth of *Doppler* spectrum) is usually relatively high. If both the transmitter and receiver are approaching a scatter that reflects the radio transmission from the transmitter to the receiver, this creates a *Doppler* shift twice the speed of a single vehicle. The situation particularly degrades when a highly mobile scatter, such as another traveling vehicle, appears. Because such situations frequently occur in this scenario, the PER will increase dramatically if no CFR prediction is performed, as with the STA and CDP schemes shown in Figure 1(c) and 2(c). Moreover, because the overall Rician K factor in this scenario is larger than that in the V2V Expressway Oncoming scenario, the proposed DDP scheme performs better than that in the latter. Even a further improved performance can be achieved by using the C-DDP scheme, as shown in Figure 2(c).

5. Implementation Issue

A reference design for the proposed DDP scheme on the FPGA platform is presented in this section, and a block diagram of it is described in Figure 3. The proposed estimator is composed of three parts: Part (1) is used to estimate the DDE vector for the currently-processing symbol; the prediction of the DDE vector for the subsequent symbol to receive is carried out in Part (2); the CFR estimation for the subsequent symbol can be obtained by using Part (3). In Part (1), the channel coefficients in the data and pilot sub-carriers are estimated and then mixed with the coefficients in the null sub-carriers obtained from the previously-received symbols, the initial values of which are estimated from the LTSs. Based on equation (5), a hardware divider is required to directly calculate the $\hat{H}_k^i$, and this results in a large amount of hardware resource consumption. Considering that only a few predefined values for the denominator $\hat{S}_k^i$ are available in a different modulation scheme, the division operation can be implemented using a multiplier if the reciprocal value of the $\hat{S}_k^i$ has been previously determined and saved. What is more, it can also be implemented using the simple logic for BPSK, because the denominator is always either 1 or -1 [12]. Next, the estimation of the DDE vector for the currently-processing symbol can be obtained by using an IFFT module.

The prediction of the DDE vector for the subsequent symbol to receive is performed in Part (2). The DDE expressed in Equation (14) is composed of two parts, which can be rewritten as

$$\begin{cases} A_m^i = \sum_{k=1}^{W} \hat{b}_m^{i-k+1} = A_m^{i-1} + \hat{b}_m^i - \hat{b}_m^{i-W} \\ B_m^i = \sum_{k=1}^{W} k\hat{b}_m^{i-k+1} = B_m^{i-1} + A_m^i - W\hat{b}_m^{i-W} \end{cases}, 0 \le m \le M \quad (15)$$

These values can be determined in an iterative way in order to reduce hardware resource usage, as shown in part (2) of Figure 3. In order to predict the CFR for the next symbol, it is necessary to maintain the DDE vectors for the latest received W OFDM symbols. The random access memory, which is denoted as RAM1 in Figure 3 and can be implemented by using the on-chip block memory or registers in the FPGA chip, is used for this operation, and the memory resource occupied by RAM1 is $2W(M+1)D_W$ bits, where D_W denotes the internal word length used in the estimator. Using a similar method, RAM2 and RAM3 in Figure 3 are used to reserve the historic A_m^i and B_m^i in the iteration process, and both of them occupy a $2(M+1)D_W$ -bit memory resource. Although three multiplication operations are involved in part (2), they can be implemented using some bitwise shifters plus adders, because the multiplicands in them (W, ω_1, and ω_2) are constant values.

The prediction of the CFR for the next symbol to receive is obtained in Part (3). The prediction of the CFR can be obtained by performing the FFT operation on the sequence, which is read as:

$$\hat{b}_{m,fft}^{i+1} = \begin{cases} \hat{b}_{m,pre}^{i+1}, & 0 \le m \le M \\ 0, & others \end{cases}, \tag{16}$$

It can be implemented by using a zero-padding module. In the end, the final prediction on the channel CFR is reserved in the RAM4 block (occupies $128\boldsymbol{D}_W$ bits memory resource), and it will be used to equalize the next symbol to receive.

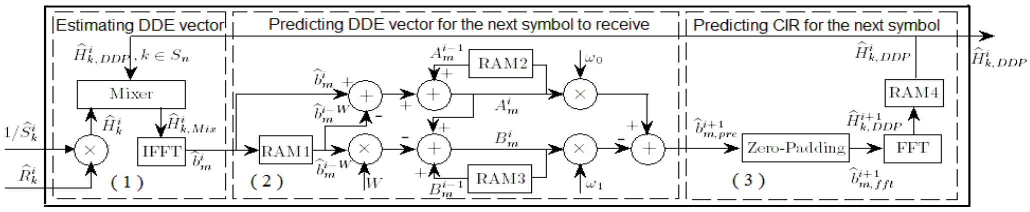

Figure 3. Block diagram of the proposed DDP estimator, where $\omega_0 = (2(2W+1))/(W(W-1))$, $\omega_1 = 6/(W(W-1))$, and RAM1-RAM4 denote the random access memory.

Table 1. Resource usage of proposed DDP scheme

Resource	Usage
Total combinational functions	2,528
Total registers	1,800
Total memory bits	10,240
Embedded Multiplier 9-bit elements	16
Estimated Total logic elements	3,011

In order to demonstrate the complexity and feasibility of the proposed scheme, we implemented it on the EP4CE115F29C chip from Altera Corporation, whose FPGAs are widely used for verifying high-speed algorithms [19]. The resource usage given by Quartus II software is shown in Table 1. Due to the similarity between the IFFT and FFT operations shown in Figure 3, they can share the identical hardware resources by time-division multiplex, and the hardware resource usage can be further reduced. Moreover, since the FFT and IFFT operations introduce too much latency, the processing latency (from input to output) of the DDP scheme is estimated to reach up to 363 clock cycles. This means that a higher clock frequency must be used to estimate the CFR for the next symbol before it arrives in the receiver.

6. Conclusion

This paper presents a practical channel estimation scheme adhering to the IEEE 802.11p standard. An enhanced DDP method was presented for estimating and predicting the dynamic propagation channel in V2V communications. In the proposed DDP method, de-mapped or decoded data are used to construct data pilots and update the CFR estimation during the receiving process. In the frequency domain, the LS method is used to average the CFR estimation for the purpose of suppressing noise; in the time domain, the linear prediction method is used to trace and predict the dynamic channel caused by the *Doppler* shift. The validity of the proposed DDP method was verified by computer simulation for three typical V2V communication scenarios. The results demonstrated that the proposed DDP method outperforms the traditional channel estimation methods in V2V communication scenarios. A reference design was also provided. The proposed DDP estimation can thus be easily implemented and has an acceptable level of complexity on the FPGA platform.

Acknowledgements

This work is supported by the Key Program of National Natural Science Foundation of China under grant 61331009.

References

[1] Kenney JB. *Dedicated short-range communications (DSRC) standards in the United States*. Proceedings of the IEEE. 2011; 99(7): 1162-1182.
[2] IEEE WG802.11 - Wireless LAN Working Group. IEEE Std 802.11p-2010*. IEEE Standard for Local and Metropolitan Area Networks - Specific requirements Part 11: Wireless LAN Medium Access Control (MAC) and Physical Layer (PHY) Specifications Amendment 6: Wireless Access in Vehicular Environments*. New York. 2010.
[3] Engels M. Wireless OFDM Systems: How To Make Them Work?. NewYork: Springer Science & Business Media. 2002.
[4] Acosta-Marum G, Ingram MA. Six time- and frequency- selective empirical channel models for vehicular wireless LANs. *IEEE Vehicular Technology Magazine*. 2007; 2(4): 4-11.
[5] Mecklenbrauker CF, Molisch AF, et al. *Vehicular Channel Characterization and Its Implications for Wireless System Design and Performance*. Proceedings of the IEEE. 2011; 99(7): 1189-1212.
[6] Speth M, Fechtel S, Fock G, Meyr H. Optimum receiver design for OFDM-based broadband transmission .II. A case study. *Communications, IEEE Transactions*. 2001; 49(4): 571-578.
[7] Coleri S, Ergen M, et al. Channel estimation techniques based on pilot arrangement in OFDM systems. *IEEE Transactions on Broadcasting*. 2002; 48(3): 223-229.
[8] Singh S, Ram H, Gill SS. Performance Evaluation of Channel Estimation in OFDM System for Different QAM and PSK Modulations. *International Journal of Electrical and Computer Engineering (IJECE)*. 2011; 1(2): 140-150.
[9] Wang Y, Zhang Z, Chen Y. Pilot-aided Joint Channel Estimation for OFDM Based Cooperative Multi-cell Networks. *TELKOMNIKA Indonesian Journal of Electrical Engineering*. 2014; 12(9): 6860-6867.
[10] Zhang Y, et al. *A differential OFDM approach to coherence time mitigation in DSRC*. Proceedings of the fifth ACM international workshop on VehiculAr Inter-NETworking. San Francisco. 2008: 1-6.
[11] Wu XZ, Subramanian S, et al. Vehicular communications using DSRC: challenges, enhancements, and evolution. *Selected Areas in Communications, IEEE Transactions*. 2013; 31(9): 399-408.
[12] Fernandez JA, Borries K, Lin C, et al. Performance of the 802.11p Physical Layer in Vehicle-to-Vehicle Environments. *Vehicular Technology, IEEE Transactions*. 2012; 61(1): 3-14.
[13] Zhao ZJ, Cheng X, et al. Channel Estimation Schemes for IEEE 802.11p Standard. *Intelligent Transportation Systems, IEEE*. 2013; 5(4): 38-49.
[14] Boumard S, Mammela A. *Channel Estimation Versus Equalization in An OFDM Wlan System*. IEEE Vehicular Technology Conference. Rhodes. 2001; 1: 653-657.
[15] Ozdemir MK, Arslan H. Channel estimation for wireless OFDM systems. *Communications Surveys & Tutorials, IEEE*. 2007; 9(2): 18-48.
[16] Zhan L, Zhang WX. The Computer Design of Practical Filter. *Journal of Digital Information Management*. 2013; 11(3): 175-178.
[17] Yang BG, Cao ZG, Letaief KB. Analysis of low-complexity windowed DFT-based MMSE channel estimator for OFDM systems. *Communications, IEEE Transactions*. 2001; 49(11): 1977-1987.
[18] Kang Y, Kim K, Park H. Efficient DFT-based channel estimation for OFDM systems on multipath channels. *Communications, IET*. 2007; 1(2): 197-202.
[19] Fan B, Tan G, Fan S. Comparison of Three Different 2-D Space Vector PWM Algorithms and Their FPGA Implementations. *Journal of Power Technologies*. 2014; 94(3): 176-189.